molecular pharmaceutics

pubs.acs.org/molecularpharmaceutics

Article

Can We Predict Clinical Pharmacokinetics of Highly Lipophilic Compounds by Integration of Machine Learning or In Vitro Data into Physiologically Based Models? A Feasibility Study Based on 12 Development Compounds

Neil Parrott,* Nenad Manevski, and Andrés Olivares-Morales

Cite This: https://doi.org/10.1021/acs.molpharmaceut.2c00350

Read Online

ACCESS | Metrics & More | Article Recommendations | Supporting Information

ABSTRACT: While high lipophilicity tends to improve potency, its effects on pharmacokinetics (PK) are complex and often unfavorable. To predict clinical PK in early drug discovery, we built human physiologically based PK (PBPK) models integrating either (i) machine learning (ML)-predicted properties or (ii) discovery stage in vitro data. Our test set was composed of 12 challenging development compounds with high lipophilicity (mean calculated log *P* 4.2), low plasma-free fraction (50% of compounds with fu,p < 1%), and low aqueous solubility. Predictions focused on key human PK parameters, including plasma clearance (CL), volume of distribution at steady state (V_{ss}), and oral bioavailability (%*F*). For predictions of CL, the ML inputs showed acceptable accuracy and slight underprediction bias [an average absolute fold error (AAFE) of 3.55; an average fold error (AFE) of 0.95]. Surprisingly, use of measured data only slightly improved accuracy but introduced an overprediction bias (AAFE = 3.35; AFE = 2.63). Predictions of V_{ss} were more successful, with both ML (AAFE = 2.21; AFE = 0.90) and in vitro (AAFE = 2.24; AFE = 1.72) inputs showing good accuracy and moderate bias. The %*F* was poorly predicted using ML inputs [average absolute prediction error (AAPE) of 45%], and use of measured data for solubility and permeability improved this to 34%. Sensitivity analysis showed that predictions of CL limited the overall accuracy of human PK predictions, partly due to high nonspecific binding of lipophilic compounds, leading to uncertainty of unbound clearance. For accurate predictions of %*F*, solubility was the key factor. Despite current limitations, this work encourages further development of ML models and integration of their results within PBPK models to enable human PK prediction at the drug design stage, even before compounds are synthesized. Further evaluation of this approach with more diverse chemical types is warranted.

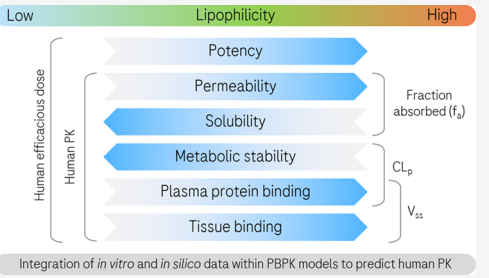

KEYWORDS: *physiologically based pharmacokinetics, lipophilicity, machine learning, drug-like properties, protein binding*

INTRODUCTION

Over the past 20 years, the prediction of clinical pharmacokinetics (PK) has moved away from empirical and nonmechanistic methods toward in vitro to in vivo extrapolation (IVIVE) embedded into physiologically based PK (PBPK) models.[1] In 2006, Jones et al.[2] published the first study demonstrating improved predictive performance of mechanistic human PBPK models compared to allometric scaling of PK parameters derived from animal species. Since then, PBPK has become firmly established as a standard technique of drug discovery and development.[3] Although PK studies in multiple animal species are no longer necessary in support of allometric scaling, uncertainties and challenges in quantitative IVIVE remain, and animal data are still frequently used to derive empirical scaling factors to support PBPK-based prediction of clearance or volume[4] or to learn about the complex interplay of drug specific and physiological factors governing in vivo absorption.[5] However, for both ethical[6] and scientific[7] reasons, the movement toward more physiologically relevant human in vitro assays continues. More advanced mechanistic in vitro tools[8−10] combined with model-based analyses[11−13] can enhance the prediction of clinical PK, while advances in the commercial PBPK modeling platforms extend their ability to integrate complexities such as transporter−enzyme interplay[14] and extrahepatic metabolism.[15] Human PBPK models may also play a role in drug discovery, when experimental data are limited.[16,17] To use PBPK models as early as possible,[18] a relevant consideration is the application of machine learning (ML) methods to predict in vitro properties related to drug absorption, metabolism, distribution, and excretion (ADME).[19] Prediction of primary human PK parameters such as CL and V_{ss}

Received: May 1, 2022
Revised: September 9, 2022
Accepted: September 9, 2022

directly from the chemical structure using ML models trained on larger data sets was recently demonstrated.[20] However, in the absence of explainable and causal ML methods,[21] this approach delivers limited mechanistic insights and does not fit with the current integrative bottom-up paradigm used in drug discovery.[18] In addition, the size of clinical PK data sets (approx. 1400 drugs[22]) sets an inherent limit to the structural diversity captured by such models, at least until transfer learning and multitask ML techniques reach maturity.[23] Use of the higher volumes of measured in vitro, human relevant, ADME data for chemical structures from industrial development pipelines offers access to a broader chemical diversity for model building, and the subsequent combination of predicted properties within a PBPK model allows simulation of concentration versus time profiles and thus prediction of primary PK parameters.[18] An additional advantage of combining ML-predicted ADME properties and PBPK models already at the early discovery stage can be the continuity that this provides with the model accompanying the compound as it progresses to the later discovery stages and then through early to late stage clinical development.[3]

The IVIVE methods are limited when molecules exhibit properties beyond the typical drug-like space, such as high lipophilicity, low metabolic turnover,[24] low free fraction in plasma (fu,p),[25] and low solubility,[26] because such properties limit the reliability of routine first-line in vitro assays or are outside the assays' dynamic range. Reliable measurements might be possible with more refined assays (e.g., see a recent review of advanced techniques for the measurement of plasma protein binding for highly bound compounds[27]), and so, ML predictions may therefore offer a valuable alternative in the future, if they can be built based on sufficiently large, accurate, and structurally diverse in vitro data sets. This paper sets out predictions of clinical PK after intravenous (IV) and oral dosing (PO) for a set of 12 Roche development compounds with extreme properties, which make prediction from in vitro data especially challenging.

The defining property of our data set is high lipophilicity (a mean calculated log *P* of 4.20; range 2.28−6.68). While high log *P* often contributes to increased pharmacodynamic potency, it also profoundly influences a number of key drug-like properties, including decreases in solubility, free fraction in plasma, and metabolic stability, as well as increases in permeability and tissue binding (Figure 1).[28,29]

Despite these challenges, the number of lipophilic drug candidates is steadily increasing across the industry, likely driven by higher difficulty and diversity of pharmacological targets.[30] Therefore, to facilitate compound selection and avoid clinical failures, early predictions of human PK for highly lipophilic compounds are important. Human PBPK models offer an ideal platform to integrate the complex effects of lipophilicity, a task that is often unfeasible by looking at individual properties, their simple ratios,[28] or ligand efficiency metrics.[31] This study describes a retrospective analysis comparing bottom-up PBPK predictions based only on ML-generated properties to those based on the first-line in vitro data measured during drug discovery. While the small size of this data set precludes strong conclusions, the clinical data evaluated are largely unpublished and therefore are unseen by the commercial ML models applied in this study.

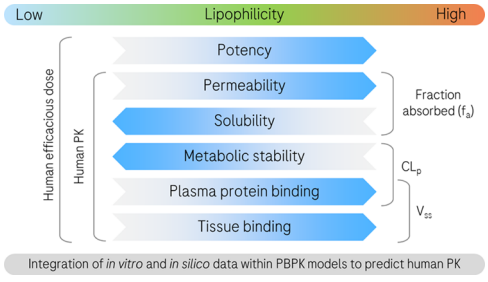

Figure 1. Modulation of lipophilicity causes complex changes in compound PK. Integrative PBPK models can provide a way to predict these effects and estimate an efficacious dose.

EXPERIMENTAL SECTION

Test Compounds and Clinical PK Data. The 12 compounds in this study were selected based on the availability of clinical PK data obtained after IV and PO dosing to healthy volunteers. Six compounds were from projects aiming at central nervous system targets, four were for the treatment of metabolic and cardiovascular disease, and two were for oncology treatments. Basic physicochemical and PK properties are presented in Table 1. The collected data were obtained from phase 1 studies performed in six to eight healthy volunteers, mostly males. The IV doses were administered as short infusions in 8 of the 12 cases as a microdose (an IV dose $\leq$ 0.1 mg) (Table S1). The PO doses were administered as capsules and tablets or as a solution in either the fasted or the fed state (Table S1).

Software. ML input parameters for the PBPK models were predicted with ADMET Predictor 10.1.0.1, and the PBPK models were developed in GastroPlus version 9.8.001. Both software applications are from Simulations Plus Inc.[32]

Modeling Strategy. The step-by-step process to construct models and assess PBPK simulations is summarized below.

1. ADMET Predictor was used to generate ML predictions for all inputs to PBPK models by loading a file of chemical structures using the *Import Structure* menu option in GastroPlus.
2. For each compound, a mean observed plasma concentration versus time profile at the given IV dose in milligrams was constructed by taking the arithmetic mean of concentrations across all individuals at each measured time point.
3. PBPK simulations were run for the specified IV dose using the default GastroPlus human male physiology. Simulated concentrations were compared to mean observed concentrations from step 2. The predicted and observed PK parameters, V_{ss} and CL, were also calculated and compared (results are presented in Figure 2A,C and Table 2 in columns headed ML).
4. ADMET Predictor estimates of fu,p, blood/plasma concentration ratio (Rb/p), and intrinsic hepatic metabolic clearance (CL_{int}) were replaced with properties measured in vitro, and simulations and assessments were repeated (results are presented in Figure 2B,D and Table 2 in columns headed in vitro).
5. For assessment of simulated oral PK, the PBPK disposition models were applied, and drug absorption was simulated with the default advanced compartmental absorption and transit (ACAT) models for either fasted or fed state human gastrointestinal physiology depending on the clinical study being predicted (Table S1).
6. For one oral dose (for dose selection criteria, see Supplementary Material—Data analysis of clinical PK

https://doi.org/10.1021/acs.molpharmaceut.2c00350
Mol. Pharmaceutics XXXX, XXX, XXX−XXX

Table 1. Basic Physicochemical and PK Properties of the 12 Test Compounds

ID	MW	log P[a]	pK_a[b,c]	Rb/p[d]	fu,p[e] (%)	CL[f] (L/h)	V_{ss}[g] (L)	P_{eff}[h] (cm/s × 10^{-4})	Aqueous solubility[i] (μg/mL)	pH for solubility	%F
1	465	4.71	2.2b, 7.1a	0.7	0.16	16.6	35	4.2	0.02	7	53
2	326	4.55	2.9b, 3.8b	0.76	1.4	8.0	1150	7.5	0.3	7	53
3	447	4.68	1.1b, 4.5b	0.76	0.10	2.3	511	1	<1	7	30
4	386	2.33	neutral	1.01	17.0	10.5	56	0.6	2600	6.8	102
5	438	3.91	8.6b	0.69	1.2	18.1	225	1.6	5	6.5	n/a
6	445	2.40	2.3b	0.59	5.6	3.8	50	3.7	10	7	72
7	463	3.93	1.5b, 11.2a	0.64	0.09	0.73	308	1.8	1	7.2	22
8	410	3.82	1.8b, 3.2b,5.6b	0.75	13.2	10.0	203	3.5	63	7	134
9	566	6.41	2.2b, 4.4b	0.65	0.10	14.4	3360	1.7	13	1	11
10	483	4.69	2.3b, 7.2b, 10.3a	2.6	0.30	31.8	469	2.5	0.019	7.3	34
11	617	6.68	11a, 4.5m, 3.6m	0.7	0.10	0.53	65	3.3	<0.05	7	13
12	363	2.28	4b	0.69	28.0	2.65	107	2.5	140	7	100

[a]ADMET Predictor. [b]ADMET Predictor: a = acid, b = base, m = mixed (mixed pK_a is assigned when an ionizable group cannot be defined as strictly acidic or basic). [c]Blood to plasma concentration ratio measured in house. [d]Fraction unbound in plasma measured in house. [e]Observed plasma clearance. [f]Observed volume of distribution. [g]Jejunal permeability scaled from Caco-2 apparent permeability. [h]Measured in buffer at the specified pH (see Table S3 for biorelevant solubility). [i]Absolute bioavailability estimated with NCA.

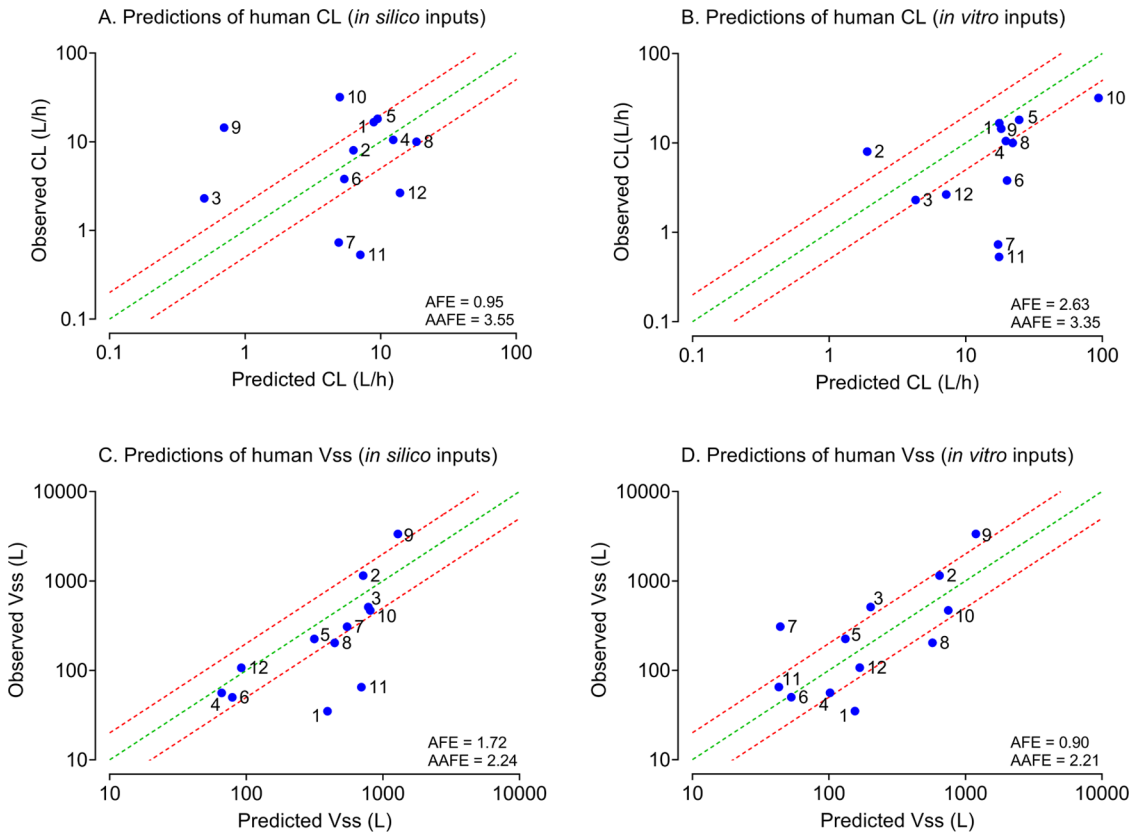

Figure 2. Predicted and observed human CL and V_{ss}. (A) CL predicted from ML inputs; (B) CL predicted from measured in vitro data (fu,p, Rb/p, and hepatocyte CL_{int}); (C) V_{ss} predicted from ML inputs; and (D) V_{ss} predicted from measured in vitro data (fu,p and Rb/p). Green and red dotted lines represent lines of unity and 2-fold prediction error, respectively.

profiles after PO administration), a single observed plasma concentration versus time profile was constructed by taking the arithmetic mean of measured concentrations at each time point across all individuals.

7. PBPK model simulations of oral PK based on only ML inputs were evaluated. Simulated concentrations were compared to mean observed concentrations. The predicted and observed PK parameters: area under the concentration versus time curve extrapolated to infinity (AUC), maximum concentration (C_{max}), and %F were also calculated and compared (Figure 3A and Table 3 column 3).
8. A 1, 2, or 3 compartmental model was fitted to the mean observed IV PK profile from step 2 and added to GastroPlus to describe systemic clearance and distribution. The hepatic first pass extraction ratio was estimated as the ratio of systemic blood clearance to liver blood flow. Intestinal metabolism was assumed to be negligible.
9. PBPK model simulations of absorption based on ML inputs for absorption were evaluated. Simulated concen-

https://doi.org/10.1021/acs.molpharmaceut.2c00350
Mol. Pharmaceutics XXXX, XXX, XXX−XXX

Table 2. Predicted and Observed PK Parameters for IV Dosing

		ML[a]	in vitro[b]		ML[a]	in vitro[b]
record number	observed CL (L/h)	predicted CL (L/h)	predicted CL (L/h)	observed V_{ss} (L)	predicted V_{ss} (L)	predicted V_{ss} (L)
1	16.6	8.9	17.6	35	393	155
2	8.0	6.3	1.9	1150	718	646
3	2.3	0.5	4.3	511	782	202
4	10.5	12.4	19.7	56	66	102
5	18.1	9.5	24.6	225	315	132
6	3.8	5.4	20.1	50	79	53
7	0.73	4.91	17.3	308	547	44
8	10	18.4	22.1	203	444	573
9	14.4	0.7	18.2	3360	1290	1190
10	31.8	5.0	93.8	469	808	748
11	0.53	7.09	17.5	65	696	43
12	2.65	13.9	7.2	107	92	168
	AFE	**0.95**	**2.63**		**1.72**	**0.90**
	AAFE	**3.55**	**3.35**		**2.24**	**2.21**
	within 2-fold	**6**	**5**		**8**	7

[a]All input parameters generated with ADMET Predictor. [b]ML inputs replaced with measured fup, Rb/p, and hepatocyte CL_{int}.

trations were compared to mean observed concentrations, and predicted and observed PK parameters were compared (Figure 3B and Table 3, column 4).

10. PBPK model simulations of absorption based on measured inputs for absorption were evaluated. Predicted aqueous solubility, biorelevant solubility, and jejunal permeability were replaced with measured properties, and simulations were repeated and re-assessed (Figure 3C and Table 3 column 5).
11. Finally, for completeness, predictions of oral PK parameters based on measured inputs for absorption and disposition were evaluated.

Calculation of PK Parameters. The GastroPlus software reports PBPK-based estimates of volume and clearance for each simulation using internal methods. However, to avoid bias, we estimated the parameters from both simulated and observed profiles using the same noncompartmental analysis (NCA) method based on mean observed plasma concentration versus time profiles and based on the simulated concentrations at the same time points as for the measured data. The PKPlus module in GastroPlus was used for the NCA and for fitting of compartmental models (step 8 above). For model fitting, an objective function weighting of $1/(y + y\_hat)^2$ was applied, and the best model was selected based on the Akaike information criterion. Model parameters are provided in Table S2.

Assessment of Predictions. Fold errors for the predicted PK parameters were estimated as below:

$$\text{fold error} = \left\{\frac{\text{predicted}}{\text{observed}}\right\}$$

Bias was assessed using the average fold error (AFE; AFE < 1 and AFE > 1 indicate underprediction and overprediction bias, respectively):

$$\text{average fold error} = 10^{\sum_{i=1}^{n} \log(\frac{\text{predicted}}{\text{observed}})/n}$$

Precision was assessed using the average absolute fold error (AAFE; value of 1 indicates perfect predictions):

$$\text{average absolute fold error} = 10^{\sum_{i=1}^{n} \text{abs}(\log(\frac{\text{predicted}}{\text{observed}}))/n}$$

For bioavailability, the average prediction error (APE) and average absolute prediction error (AAPE) were used, where average refers to the arithmetic mean and where

$$\text{prediction error} = \{\text{observed bioavailability} - \text{predicted bioavailability}\}$$

ML-Predicted PBPK Model Inputs. A GastroPlus database was created by importing chemical structures contained in a structure-data file (*.SDF). The default ML models were taken to generate properties by accepting the "Use Predicted" option and choosing a PBPK model for disposition. For the PBPK model, the Population Estimates for Age-Related Physiology (PEAR physiology) for a 30 year-old American male [86 kg, body mass index (BMI) = 27.5] was used for all compounds irrespective of the actual clinical population. This was considered most appropriate to represent the situation where a human PK prediction is made prior to the detailed knowledge of the demographics of the actual population in the first-in-human (FIH) study.

The ADMET Predictor-predicted properties used models as described below. Rb/p values were predicted using the RBP model (trained on data for 204 molecules), fu,p values were predicted with the hum_fup% model (trained on data for 1986 molecules), and intrinsic clearance used the CYP_HLM_CLint model which predicts an unbound intrinsic clearance and was trained on measured data for apparent CL_{int} corrected for binding using the S + fumic model. The octanol−water partition coefficient was predicted with the S + log *P* model trained on 12,820 experimental values. Aqueous solubility predictions used the S + Sw model for native solubility trained on data for 3596 compounds, while biorelevant solubility in FaSSIF and FeSSIF used the S + FaSSIF and S + FeSSIF models (trained with data for 160 compounds). Ionization constants came from the S + pK_a model which was trained on data for over 25,000 measured pK_a values. Finally, effective permeability in human jejunum was predicted with the S + P_{eff} model.

Drug distribution was modeled using perfusion-limited tissues with tissue partition coefficients predicted with the Lukacova (Rodgers single) option.[33,34] For the calculation of the partition coefficients which describe distribution into tissues, the "Use Adjusted" option was selected for the plasma unbound fraction,

https://doi.org/10.1021/acs.molpharmaceut.2c00350
Mol. Pharmaceutics XXXX, XXX, XXX−XXX

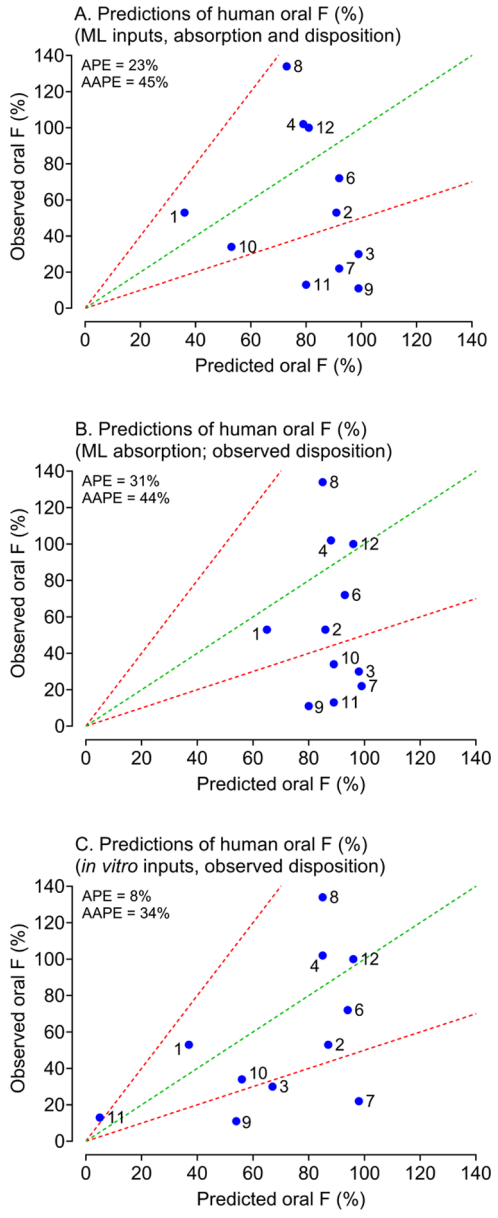

Figure 3. Predicted and observed %*F*. (A) All PBPK model inputs predicted with ML; (B) observed data after intravenous dosing used to model postabsorptive processes, permeability, and solubility predicted with ML; and (C) observed data after intravenous dosing used to model postabsorptive processes, measured solubility, and permeability used to predict absorption. Green and red dotted lines represent lines of unity and 2-fold prediction error, respectively.

fup_adj. This accounts for drug partitioning into plasma lipids based on the log *P* of the molecule and the lipid composition of human plasma assuming that fu,p measures only drug binding to plasma proteins.[35]

$$\mathrm{fup_{adj}} = \frac{1}{\left(\frac{V_{\mathrm{lipid}}}{V_{\mathrm{water}}}\right)10^{\log P} + 1 + \frac{1-\mathrm{fup}}{\mathrm{fup}}}$$

where V_{lipid} is the volume fraction of total neutral lipid and phospholipid in plasma (taken as 0.00575) and V_{water} is the volume fraction of water in plasma (taken as 0.945).

Biotransformation analysis showed that our compounds predominantly undergo oxidative metabolism (data not shown). Therefore, we considered that ML models trained on in vitro data from either human liver microsomes (HLMs) or human hepatocytes (HHEP) could be appropriate. According to the validation statistics provided in the ADMET Predictor manual, the HLM and HHEP models have similar performance. We evaluated both models and found comparable results (see Figure S7). For simplicity, we only used the HLM model in this work.

The CYP_HLM_CLint model predicts $\mathrm{CL_{int}}$ in μL/min/mg protein and was built with in vitro intrinsic clearances measured in HLMs for a set of 1590 molecules. This model is labeled as the "total liver microsome" model in the GastroPlus import options. The $\mathrm{CL_{int}}$ value was converted to in vivo based on a microsomal protein content of 38 mg protein/g tissue and a liver weight of 1827 g. Thus, intrinsic unbound clearance in L/h is given by

$$\text{unbound in vivo } \mathrm{CL_{int}(L/h)} = \frac{\mathrm{CL_{int}} \times 38 \times 1827}{(10^6/60)}$$

The in vivo hepatic plasma clearance was then predicted with the well-stirred liver model based on the predicted unbound intrinsic clearance, the predicted fu,p, and the predicted B/P with a hepatic blood flow of 94 L/h taken from the default GastroPlus physiology.

For the simulation of oral absorption based on ML inputs, default predicted properties were taken for all model parameters. For solubility, thermodynamic solubility in water and the corresponding pH were combined with predicted ionization constants and solubility factors to estimate a solubility versus pH profile which was then combined with predicted biorelevant solubilities (FaSSIF and FeSSIF) to estimate a bile salt solubilization ratio (BSSR) (Table S3). The default precipitation time of 900 s was retained for all molecules, but the default particle diameter of 50 μm was reduced to 10 μm as more realistic for the typical micronized formulation used in phase 1 clinical studies.

ADMET Predictor also uses the ionization, permeability, and molecular weight of molecules to predict the likely clearance pathways according to the extended clearance classification system (ECCS),[36] and this was also assessed in this study.

Measured In Vitro Properties. The fu,p was measured in human plasma, and Rb/p was measured in freshly drawn blood. Intrinsic metabolic clearance was determined based on the loss of the parent compound measured after incubation of the test compound with human hepatocytes. The in vitro assays are described more fully in Kratochwil et al.[24] Permeability was measured in Caco2 cells (pH 6.5 on the apical to pH 7.4 on the basolateral side) and converted to human jejunal permeability based on a correlation for reference drugs as described in Parrott and Lave.[37] Solubility was measured in aqueous buffer and also in biorelevant media.[37]

For prediction of CL, the apparent intrinsic clearance measured in hepatocytes (in vitro $\mathrm{CL_{int}}$ μL/min/10^6 cells) was scaled to account for liver weight (1827 g) and hepatocellularity (120×10^6 hepatocytes per gram of liver) as shown below:

$$\text{unbound in vivo } \mathrm{CL_{int}(L/h)} = \frac{\text{in vitro } \mathrm{CL_{int}} * \text{hepatocellularity} * \mathrm{LW}}{\mathrm{fu_{incubation}} * (10^6/60)}$$

The suspension hepatocyte assay is performed with a medium containing protein (10% fetal calf serum), and our default

https://doi.org/10.1021/acs.molpharmaceut.2c00350
Mol. Pharmaceutics XXXX, XXX, XXX−XXX

Table 3. Predicted and Observed %F for Oral Dosing

		predicted %F			
compound	observed %F	ML disposition inputs and ML absorption inputs	measured input data for disposition inputs and measured data for absorption inputs	ML absorption inputs and compartmental disposition model fitted to observed IV data	measured absorption inputs and compartmental disposition model fitted to observed IV data
1	53	36	38	65	37
2	53	91	97	86	87
3	30	99	64	98	67
4	102	79	76	88	85
5	n.a.				
6	72	92	60	93	94
7	22	92	69	99	98
8	134	73	67	85	85
9	11	99	51	80	54
10	34	53	52	89	56
11	13	80	4	89	5
12	100	81	89	96	96
	APE	**23%**	**4%**	**31%**	**8%**
	AAPE	**45%**	**30%**	**44%**	**34%**
	within 20%	**4**	**5**	**3**	**4**

scaling approach, based on previous experience with our in-house assay, is to assume that the fraction unbound in the incubation (fu,inc) is the same as fu,p. However, an approach where the fu,inc was calculated assuming a dilution effect due to only 10% FCS in the medium was also explored.[38] Scaling to in vivo clearance then used the well-stirred model as described for the ML-predicted CL_{int}. Extrahepatic metabolic clearance and transporter-mediated clearance were assumed negligible for all the simulations performed in this study. This was necessary since neither relevant ML models nor in vitro data were available for this data set.

RESULTS

Observed Properties of Test Compounds. Basic physicochemical and PK properties of test compounds are shown in Table 1. A majority of compounds were basic (70% with basic pK_a >3), with compounds **5** and **10** showing strong basic pK_a values > 7. Compounds **4**, **6**, and **7** were predominantly neutral, compound **1** was acidic, and compound **11** was zwitterionic. All compounds are highly lipophilic, with predicted log *P* values ranging from 2.3 to 6.7 and an average of 4.2. Measured binding to plasma proteins is high with half of the compounds exhibiting a fu,p < 1%. Observed CL values are low, with an average CL of only 10 L/h (a geometric mean of 5.6 L/h) and values ranging from extremely low (<1 L/h) to moderate (32 L/h). Observed V_{ss} volumes are also high with an average of 550 L (a geometric mean of 213 L), and two compounds (**2** and **9**) exhibit extremely large volumes beyond 1000 L. Permeability is moderate to high for all compounds (an average P_{eff} of 2.83 cm/s × 10^{-4}), but measured aqueous solubilities are low and only two compounds show a dose number < 1 (where the dose number is the ratio of the dose to the amount that can be dissolved in 250 mL at the lowest aqueous solubility between pH 1 and pH 8). Despite low aqueous solubilities, the observed oral bioavailabilities are reasonably high with an average of 57% and a range from 11 to 134%.

ADMET Predictor-predicted metabolism to be the major clearance pathway for most of the molecules (Table S4). According to the predicted ECCS categories, 67% of compounds were class 2 and likely to be cleared via metabolism, two compounds (**3** and **9**) were class 4, where renal clearance is likely to be important, and the remaining two compounds were in classes 1B and 3B, where active uptake is predicted to play a role in hepatic clearance. In fact, the observed clinical data showed only minor renal elimination (<2%) for all compounds except for compounds **4** and **12**, which showed, respectively, fractions of dose in the urine of 16 and 11%.

Comparison of ML-Predicted and Experimental Inputs. Due to the high lipophilicity of test compounds, measurements of log *D* were only possible for a subset with lower values (log $D \leq 4$). However, the estimates of log *P* based on measurement showed good alignment with the ML-predicted values (Table S5). Similarly, the measured ionization constants were comparable to ML predictions (Table S6).

Predicted fu,p values showed marked overprediction bias compared to measurements (an AFE of 5.89; an AAFE of 9.02), especially when the measured fu,p was less than 1% (Table S7, Figure S1). ADMET Predictor estimated fu,p > 1% for all molecules, whereas 6 out of 12 test compounds showed measured fu,p < 1%. Adjustment for partitioning into plasma lipids significantly improved predictions of fu,p, reducing the overprediction bias and improving the overall precision (an AFE of 1.32; an AAFE of 4.57).

The Rb/p was well predicted, with minimal underprediction bias and good precision (an AFE of 0.92; an AAFE of 1.22) (Table S8). An exception to this trend was compound **10**, which was underpredicted by 3.5-fold (measured 2.6 vs predicted 0.76).

Permeability was well predicted (Table S3). The AFE was 1.2, and the largest fold error was a 3.9-fold overprediction for compound 3. Biorelevant solubilities tended to be overpredicted with the largest fold errors of 40 and 47 in the FeSSIF predictions for compounds **3** and **11**, respectively. The AFE across all biorelevant solubility predictions was 2 with FeSSIF tending toward higher overprediction (an AFE of 3) than FaSSIF (an AFE of 1.2).

Predictions of PK after an IV Dose. Predicted human CL and V_{ss} parameters are compared to the observed values in Table 2 and Figure 2.

Prediction of CL based on ML inputs showed a slight underprediction bias with an AFE of 0.95, but precision was poor with an AAFE of 3.55 and only half of the predictions

https://doi.org/10.1021/acs.molpharmaceut.2c00350
Mol. Pharmaceutics XXXX, XXX, XXX−XXX

within 2-fold of observations (Figure 2A). Considering CL categories of low (<30 L/h), medium (30−60 L/h), and high (>60 L/h), 11 out of 12 test compounds were correctly classified as low CL with only compound **10** misclassified as low when observed CL was moderate.

Use of measured in vitro data as model inputs (fu,p, Rb/p, and hepatocyte CL_{int}), with an assumption of fu,inc = fu,p, only slightly improved precision (an AAFE of 3.35) and introduced an overprediction bias (an AFE of 2.63) (Figure 2B). Only five of the predictions were within 2-fold of observed, while 11 molecules were correctly classified as low CL. Again, compound **10** was incorrectly classified being predicted as high instead of moderate CL.

In vitro CL_{int} was also scaled using a calculated fu,inc, assuming a dilution of plasma to 10% of protein concentration. This "plasma dilution" scaling method slightly improved overall precision (an AAFE of 3.04) but introduced an underprediction bias (an AFE of 0.59), with five predictions within 2-fold from observations (Figure S2 and Table S9). However, considering a subset of six compounds with fu,p < 1%, the dilution method gave overall better predictions especially for compounds **7** and **11**, which had fold errors reduced to 3- and 6-fold, respectively, compared to >20-fold errors when assuming fu,inc = fu,p.

Using ML inputs and adjusting the fu,p for plasma lipid partitioning, the human V_{ss} was more accurately predicted than CL with an AFE of 1.72, an AAFE of 2.24, and eight of predicted values within 2-fold of observed (Figure 1C). Substituting Rb/p and fu,p with measured values reduced the overprediction bias (an AFE of 0.90), while overall precision remained similar (an AAFE of 2.21) and seven of the predicted values within 2-fold. Omitting the adjustment of measured fu,p for lipid partitioning gave a slightly worse predictions (an AFE of 1.41, an AAFE of 2.58, and five within 2-fold) (Table S10).

Prediction of plasma concentrations was also evaluated by comparing the measured concentrations to simulated values for the same time points. The PBPK-simulated profiles based on ML inputs showed an AFE of 0.63, AAFE was 3.30, and 54% of simulated concentrations were within 2-fold of observed (Figure S3).

Predictions of PK after a PO Dose. Using ML inputs only, human %*F* was poorly predicted with APE and AAPE values of 23 and 45%, respectively (Figure 3A, Table 3).

Similarly, predicted concentration−time profiles showed AAFE values of 3.89 and 2.68 for AUC and C_{max}, respectively (Tables S11 and S12; Figure S4).

Replacing ML inputs with observed IV PK data resulted in comparable predictions of %*F* (Figure 3B, Table 3; an APE of 31%, an AAPE of 44%), but predictions of AUC and C_{max} were modestly improved, with AAFE values of 2.16 and 2.60, respectively (Tables S11 and S12; Figure S5). Further replacements of solubility and permeability with measured data improved predictions of oral %*F*, with reduced bias (an APE of 8%) and better precision (an AAPE of 34%) (Figure 3C; Table 3). Consequently, predictions of AUC and C_{max} were also improved, with AAFE values of 1.89 and 1.99, respectively (Tables S11 and S12; Figure S6).

For completeness, simulations using in vitro data for both absorption and disposition were performed (Tables 3, S11, and S12). Predictions of oral AUC showed a high AAFE value of 4.4 (largely due to the low prediction accuracy of systemic clearance from in vitro data where AAFE was 3.35, Table 2). However, C_{max} was comparably well predicted with an AAFE of 2.4 and 7 compounds predicted within 2-fold of observed C_{max}.

Lastly, to explore possible explanations for significant mismatches between simulated and observed absorption profiles, a model parameter sensitivity analysis was applied for each compound. Permeability was a sensitive parameter for two compounds (**4** and **12**) and improved predictions of C_{max}. For compound **12**, a reduction in permeability from 2.5 to 0.5 cm/s $\times 10^{-4}$ was needed, while for compound **4**, an increase from 0.6 to 4.6 cm/s $\times 10^{-4}$ improved the match to observed data. For compound **2**, there was low sensitivity to solubility, dissolution rate (or particle size), and permeability, but an increased first pass extraction by 30% was found to bring the simulations better in line with observed data. For compound **8**, the *F* of 134% based on NCA reflected nonlinearity in the PK, which could not be captured in the current models. The remaining seven compounds all showed sensitivity to solubility and/or dissolution rate, which could lead to the underprediction (compounds **1** and **11**) or overprediction (compounds **3**, **6**, **7**, **9**, and **10**) of %*F*. However, other factors may play a role; for example, compounds **6** and **9** are weak bases where gastric solubility and precipitation could be important, while for compounds **3** and **7**, the model predicted a large amount of colonic absorption, resulting in over estimation of plasma exposures.

DISCUSSION

As shown in Figure 1, lipophilicity influences ADME in complex overlapping ways, and PBPK models can be a valuable tool to explore how changes propagate to overall PK.[39]

As added lipophilicity often increases the pharmacodynamic potency, many drug design teams aim for the highest log *P* allowed by good PK.[28] The idea that the log *P* should be finely balanced between the potency and PK is partially captured by the lipophilic ligand efficiency (LLE = pIC50 − log *P*), a simple metric that is often used in drug discovery.[31,40] Changes in log *D* influence many drug properties simultaneously, including solubility, permeability, metabolic stability, and binding to tissues and plasma proteins, and all of these properties influence drug PK (Figure 1). Therefore, instead of simple metrics like LLE, integrative methods are preferred to predict these complex outcomes and facilitate drug design. Prediction of human PK can be achieved by integrating drug properties into PBPK models.[2] However, when log *D* is high, measurement of these influential properties is challenging and predictions become more uncertain. In this study, we have explored, for a set of lipophilic compounds, prediction of human PK using PBPK models based on early measured ADME data or purely ML-predicted properties. The overall PK properties of the 12 compounds in the current study may be compared to the properties of 1352 drugs collected by Lombardo et al.[22] Clearances in the current study are all below 32 L/h, and the mean is only 10 L/h, while the mean of the Lombardo data set was 51 L/h. Conversely, mean V_{ss} for this data set is very high at 550 L compared to 266 L for Lombardo's data set. These observed PK properties are determined by intrinsic physicochemical and biochemical properties of the molecules. The median molecular weight and log *P* for this data set are 446 and 4.2, respectively, which are noticeably higher than the median values of 371 and 2.0 for Lombardo's data set. Further, half of our compounds have fu,p < 1%, which is the case for only 12% of Lombardo's compounds. Therefore, these compounds represent an extremely lipophilic chemical space for drug-like molecules which can be particularly challenging experimentally and for IVIVE. Protein binding is a fundamental PK property

https://doi.org/10.1021/acs.molpharmaceut.2c00350
Mol. Pharmaceutics XXXX, XXX, XXX−XXX

which influences both clearance and distribution as well as pharmacodynamics, drug-interaction potential, and toxicity. Compounds with a fu,p < 1% are associated with measurement uncertainty, and although very low free fractions can be measured,[38] regulatory agencies still refrain from recognizing values less than 1%.[41] When analyzing measured protein binding for drug discovery molecules, Gleeson reported that although higher plasma protein binding is associated with acidic compounds, binding increases with log *P* for all ionization classes.[42] The six compounds which showed extremely low fu,p in this study are not acids but highly lipophilic zwitterionic or basic molecules (log *P* ranging from 3.9 to 6.7). This places them outside the range covered by the training sets used for most in silico models and probably explains the poor predictions of fu,p seen in this study when using the artificial neural network model in ADMET Predictor since that model was trained on data with very few fu,p values <1% (ADMET Predictor reference manual). However, the ML predictions of fu,p were greatly improved by accounting for drug partitioning into plasma lipids based on the log *P*, and this eventually resulted in quite good prediction of V_{ss} based on only ML-predicted inputs. No mechanistic interpretation of the improvement in ML predictions of fu,p is implied. Rather, improvement in the ML model for fu,p should be possible via expansion of the training set used to build the model, especially to include more compounds with high log *P* values. The correction of fu,p used in this study is designed as a method to improve the prediction of tissue distribution by considering partitioning into plasma lipids. Our previous investigations[35] of V_{ss} prediction in rat showed that the Rodgers and Rowland[33,34] method tends to overpredict V_{ss} for highly lipophilic compounds, and we hypothesize that this could be due to the inability of in vitro experiments to correctly capture binding of drug to plasma lipids in vivo. The equation presented in this article therefore corrects the experimental fu,p for binding to plasma lipids assuming that the experimental fu,p is an accurate estimate of drug binding to plasma proteins and that log *P* can be used to predict drug partitioning to plasma lipids. This correction did give a slight improvement in the human V_{ss} which supports the previous finding for the rat. However, further investigation of this mechanism is necessary.

V_{ss} prediction was also reasonable when measured fu,p was used as an input. Plasma includes only a low volume fraction of lipids (<1%);[43] however, when a molecule has a very high log *P*, the partitioning into lipids can become significant and prediction of drug distribution can be improved when this is accounted for by adjustment of fu,p as seen in this study and in previous reports.

Regardless of whether ML or in vitro inputs were used, predictions of human CL were quantitatively poor with AAFE values of 3.55 and 3.35, respectively, and limited correlation between predictions and observations (Figure 2A,B). Considering first the ML model, the ADMET Predictor HLM_CLint model for hepatic metabolism was based on in vitro intrinsic clearances measured in HLMs for a set of 1590 molecules, and the root mean squared error for the model was 0.43 log units. The 12 molecules in this data set are believed to be mainly cleared via oxidative metabolism, and so, underprediction due to neglecting nonoxidative or extrahepatic routes may be relatively minor. However, prediction of systemic clearance from unbound intrinsic clearance requires correction for the free fraction, both in vitro and in vivo, and this can be expected to introduce a significant additional error for these very highly bound drugs. Furthermore, the set of molecules used to train the HLM_CLint model may not have included many molecules with such high log *P*. Other approaches have been described to build ML models to predict in vivo systemic clearance directly; for example, Berellini reported on a linear partial least-squares model using physicochemical descriptors and structural fragments and trained on a data set of systemic clearances for 754 compounds.[44] Their model validation showed a geometric mean fold error (GMFE) of 2.1 with 59% of compounds predicted within 2-fold. More recently, Wang et al.[20] reported even better predictions with a RMSE of 0.103 for CL predictions based on a random forest ML method trained on Lombardo's data set of 1352 drugs.

Surprisingly, the use of measured CL_{int}, fu,p, and Rb/p data failed to significantly improve the predictions of CL for this data set (Figure 2B). This may be related to several factors. For example, the suspension hepatocyte assay used is known to be limited in precision when determining CL_{int} values less than 3 μL/min/10^6 cells.[8] This applies for 9 out of 12 compounds in this study, and it is likely that use of a more precise assay for low CL_{int} measurement would give better results, for example, a long-term hepatocyte culture.[10,24] However, it is acknowledged that at the drug discovery stage, the higher cost of such assays limits their use to particularly interesting compounds, and the suspension assay is a more realistic option for higher throughput.[10] Another contributing factor to the poor IVIVE for clearance is a high amount of nonspecific binding due to high log *P*, which limits the accuracy of the determined unbound CL_{int} values. A recent cross-industry analysis supported by the International Consortium for Innovation and Quality in Pharmaceutical Development showed how poor prediction of clearance can be the result of inaccurate estimation of fu,inc for lipophilic compounds with log *P* >3[45] and also showed that use of ML models developed using proprietary data sets can better predict fu,inc for compounds with high lipophilicity. Although the focus of this work is on prediction prior to the first clinical dosing, once clinical development has started an early study arm where an oral dose is given simultaneously with an intravenous microdose (as done for 8 of 12 compounds here) can be valuable when the human clearance is highly uncertain as it can rapidly elucidate the causes of low exposures (e.g., to guide formulation work for low solubility drugs). Likewise, availability of actual demographic data for the studied populations can be used to replace generic physiological model parameters, although this is not likely to be a significant source of error for this study since the study demographics were close to the assumed generic settings of a 30 year-old male with a body weight of 86 kg and a BMI of 27.5 (see Table S1).

Regarding renal clearance, this study assumed that these lipophilic molecules with low free fraction in plasma would show negligible renal excretion, and this was largely confirmed by the clinical data, although the two least lipophilic molecules, **4** and **12**, did show minor renal clearance (Table S4).

Partitioning into blood cells is important to account for in physiological model-based clearance prediction[46] and also in prediction of V_{ss} for moderate-to-strong bases where it is used to estimate affinity to tissue acidic phospholipids[47] and becomes, in addition to fu,p, a critical parameter for accurate V_{ss} prediction.[39] In this study, only compound **10** showed a poorly predicted Rb/p value, with a prediction of 0.76 compared to a measurement of 2.6. As compound **10** is a strong base, this change in Rb/p results in close to 2-fold changes in both clearance and V_{ss}, showing the potential importance of accurate prediction of this model input. The ADMET Predictor model was built based on human data

https://doi.org/10.1021/acs.molpharmaceut.2c00350
Mol. Pharmaceutics XXXX, XXX, XXX−XXX

for 204 compounds. Only few predictive models for Rb/p have been published.[48]

In this study, using only ML predictions as input parameters, V_{ss} predictions were significantly more accurate than CL predictions (AAFE of 2.24 and 3.55, respectively). This may be due to the fact that for lipophilic compounds with good membrane permeability, V_{ss} is a function of differential partitioning between plasma and tissues and so is driven by physicochemical properties and can be well captured by the tissue composition equations implemented in PBPK models.[39] This is further supported by the recent work of Nagar and Korzekwa who have taken a detailed mechanistic structure orientation-based approach to predict drug−membrane interactions and membrane partitioning which can subsequently be combined with plasma protein binding data to predict V_{ss}.[49] The notable exception to the accurate V_{ss} predictions for this data set was compound **1**, where the V_{ss} was approximately 9-fold overpredicted. A sensitivity analysis showed that this prediction is strongly affected by both the acidic pK_a value and the log *P*. Changing the pK_a from 7.1 to 6.5 or changing log *P* from 4.7 to 4.1 brings the predicted V_{ss} into agreement with the observed value.

Considering the predictions of oral PK, if only ML inputs are used, predictions of human %*F* (AAPE of 45%), AUC (AAFE of 3.89), and C_{max} (2.68) are rather poor. Even when using the observed disposition data (derived after IV dosing), predicted %*F* based on ML inputs for absorption was poorly predicted with a large AAPE of 44%. Use of measured data for permeability and solubility improved the %*F* predictions, but the remaining AAPE of 34% confirms the difficulty to predict oral absorption for poorly soluble compounds with sensitivity to multiple factors, including pH dependency and the effect of biorelevant medium composition.

Even if predictions of human PK for highly lipophilic compounds are challenging, our results show that early insights are possible with limited experimental data or, importantly, only with ML methods. The integration of ML predictions within PBPK models also enables human PK predictions at the drug design stage, even before the compounds are synthesized. Given the availability of high-throughput PBPK approaches with reduced computational requirements, this approach is now feasible.[18] From this perspective, if applied to libraries of virtual compounds, observed AAFE values of 2- to 4-fold (for V_{ss} and CL, respectively) may help with design prioritization. The feasibility of application of high-throughput PBPK for virtual libraries was demonstrated in our recent work. Similarly, the ML predictions of oral PK for %*F* (an AAPE of 45%), AUC (an AAFE of 3.89), and C_{max} (an AAFE of 2.68), while clearly insufficiently accurate for later stages, may help teams to make difficult decisions during an early stage when experimental data are missing. Despite existing limitations, compared to simple efficiency metrics (e.g., LLE) and empirical guidelines (e.g., Lipinski's rule of 5), the approach of combining ML predictions within PBPK models may offer improvements in design of lipophilic compounds. Once the compounds are synthesized, our results indicate that accurate measurements of solubility, CL_{int}, and fu,p are the key for improved PBPK model prediction accuracy. Taken together, authors recommend a twofold approach toward the future of early human PK predictions for lipophilic compounds: (1) at the drug design stage, we should invest in ML models to improve the prediction accuracy and expand applicability domains and (2) after compound synthesis, we should invest in quality in vitro assays, especially to accurately capture solubility, metabolic clearance (especially if <3 μL/min/10^6 cells), and nonspecific binding to plasma proteins (fu,p) and incubation matrices (fu,inc).

CONCLUSIONS

This evaluation of prediction of human PK for 12 compounds is too limited to draw strong conclusions. However, for highly lipophilic molecules, this study illustrates the limitations related to the measurement of in vivo relevant unbound clearance and solubility at the early discovery stage. Further evaluation of this approach with more diverse chemical types is warranted.

ASSOCIATED CONTENT

Supporting Information

The Supporting Information is available free of charge at https://pubs.acs.org/doi/10.1021/acs.molpharmaceut.2c00350.

Supplementary methods; data analysis of clinical PK profiles after PO administration; ensuring correct comparison of PK parameters derived from predicted concentrations with those based on observed concentrations; comparison of PBPK-predicted V_{ss} and V_{ss} estimated with NCA; estimation of observed bioavailability; clinical dosing in PK studies with IV and PO administration; parameters for compartmental models fit to intravenous plasma versus time concentrations; ML-predicted and measured inputs for human permeability and solubility; assignment of compounds to categories in the extended clearance categorization system; comparison of predicted log *P*, log *D* pH 7.4, and measured log *D* pH 7.4; comparison of measured and predicted ionization constants; predicted and measured human fu,p values; predicted and measured blood-to-plasma ratios (Rb/p); prediction of CL using apparent CL_{int} adjusted for calculated fu,inc assuming a dilution of plasma proteins to 10% (the "plasma dilution" scaling method); prediction of human V_{ss} using measured fu,p and Rb/p without fu,p adjustment; observed and predicted AUCinf values after PO dosing; observed and predicted C_{max} values after PO dosing; predicted and measured human fu,p; prediction of CL using apparent CL_{int} adjusted for calculated free fraction in the incubations assuming dilution of plasma proteins to 10%; observed and PBPK model-predicted plasma concentrations for IV doses of 12 compounds using ML for all model inputs; prediction of AUC and C_{max} using ML predictions for all absorption and disposition inputs; prediction of AUC and C_{max} using ML predictions for absorption and compartmental disposition models fit to observed data; prediction of AUC and C_{max} using measured inputs for prediction of absorption and compartmental disposition models fit to observed data; comparison of predictions of clearance using ML models based on either HLM data or human hepatocyte data; mean clinical PK profiles after IV administration; and mean clinical PK profiles after PO administration (PDF)

AUTHOR INFORMATION

Corresponding Author

Neil Parrott − *Pharmaceutical Sciences, Pharma Research and Early Development, Roche Innovation Center Basel, F. Hoffmann-La Roche Ltd., CH-4070 Basel, Switzerland;*

https://doi.org/10.1021/acs.molpharmaceut.2c00350
Mol. Pharmaceutics XXXX, XXX, XXX−XXX

orcid.org/0000-0001-6821-7714;
Email: neil_john.parrott@roche.com

Authors

Nenad Manevski − *Pharmaceutical Sciences, Pharma Research and Early Development, Roche Innovation Center Basel, F. Hoffmann-La Roche Ltd., CH-4070 Basel, Switzerland*

Andrés Olivares-Morales − *Pharmaceutical Sciences, Pharma Research and Early Development, Roche Innovation Center Basel, F. Hoffmann-La Roche Ltd., CH-4070 Basel, Switzerland;* orcid.org/0000-0001-9959-0810

Complete contact information is available at:
https://pubs.acs.org/10.1021/acs.molpharmaceut.2c00350

Notes

The authors declare the following competing financial interest(s): All authors are employees of F. Homann La-Roche Ltd.

■ ABBREVIATIONS

AAFE, average absolute fold error; ADME, absorption, distribution, metabolism, and excretion; AFE, average fold error; AUC, area under the concentration−time curve extrapolated to infinity; BMI, body mass index; CL, plasma clearance; CL_{int}, intrinsic metabolic clearance measured in vitro; ECCS, extended clearance classification system; FaSSIF, fasted state simulated intestinal fluid; FCS, fetal calf serum; FeSSIF, fed state simulated intestinal fluid; *F*, bioavailability after oral drug administration; Fg, fraction escaping intestinal extraction; Fh, fraction escaping hepatic extraction; fu,inc, fraction unbound in incubation; fu,p, fraction unbound in human plasma; IV, intravenous drug dosing; IVIVE, in vitro—in vivo extrapolation; LLE, lipophilic ligand efficiency; NCA, noncompartmental analysis; PBPK, physiologically based pharmacokinetics; PO, per os (oral drug dosing); Rb/p, blood-to-plasma concentration ratio; V_{ss}, volume of distribution at steady state

■ REFERENCES

(1) Rostami-Hodjegan, A. Physiologically Based Pharmacokinetics Joined With In Vitro−In Vivo Extrapolation of ADME: A Marriage Under the Arch of Systems Pharmacology. *Clin. Pharmacol. Ther.* **2012**, *92*, 50.

(2) Jones, H.; Parrott, N.; Jorga, K.; Lavé, T. A Novel Strategy for Physiologically Based Predictions of Human Pharmacokinetics. *Clin. Pharmacokinet.* **2006**, *45*, 511−542.

(3) Jones, H.; Chen, Y.; Gibson, C.; Heimbach, T.; Parrott, N.; Peters, S.; Snoeys, J.; Upreti, V.; Zheng, M.; Hall, S. Physiologically Based Pharmacokinetic Modelling in Drug Discovery and Development: A Pharmaceutical Industry Perspective. *Clin. Pharmacol. Ther.* **2015**, *97*, 247.

(4) Miller, N. A.; Reddy, M. B.; Heikkinen, A. T.; Lukacova, V.; Parrott, N. Physiologically Based Pharmacokinetic Modelling for First-In-Human Predictions: An Updated Model Building Strategy Illustrated with Challenging Industry Case Studies. *Clin. Pharmacokinet.* **2019**, *58*, 727.

(5) Pade, D.; Jamei, M.; Turner, D. B.; Mistry, B.; Martinez, M. N. Danazol oral absorption modelling in the fasted dog: An example of mechanistic understanding of formulation effects on drug pharmacokinetics. *Eur. J. Pharm. Biopharm.* **2019**, *141*, 191−209.

(6) Hansen, L. A.; Kosberg, K. A. Ethics, Efficacy, and Decision-making in Animal Research. In *Animal Experimentation: Working Towards a Paradigm Change*; Brill: 2019; pp. 275−288.

(7) Ram, R. Extrapolation of Animal Research Data to Humans: An Analysis of the Evidence. In *Animal Experimentation: Working Towards a Paradigm Change*; Brill: 2018; pp. 341−375.

(8) Docci, L.; Parrott, N.; Krahenbuhl, S.; Fowler, S. Application of New Cellular and Microphysiological Systems to Drug Metabolism Optimization and Their Positioning Respective to In Silico Tools. *SLAS Discovery* **2019**, *24*, 523−536.

(9) Fowler, S.; Chen, W. L. K.; Duignan, D. B.; Gupta, A.; Hariparsad, N.; Kenny, J. R.; Lai, W. G.; Liras, J.; Phillips, J. A.; Gan, J. Microphysiological systems for ADME-related applications: current status and recommendations for system development and characterization. *Lab Chip* **2020**, *20*, 446−467.

(10) Umehara, K.; Cantrill, C.; Wittwer, M. B.; Di Lenarda, E.; Klammers, F.; Ekiciler, A.; Parrott, N.; Fowler, S.; Ullah, M. Application of the Extended Clearance Classification System (ECCS) in Drug Discovery and Development: Selection of Appropriate In Vitro Tools and Clearance Prediction. *Drug Metab. Dispos.* **2020**, *48*, 849−860.

(11) Heikkinen, A. T.; Korjamo, T.; Lepikkö, V.; Mönkkönen, J. Effects of Experimental Setup on the Apparent Concentration Dependency of Active Efflux Transport in in Vitro Cell Permeation Experiments. *Mol. Pharmaceutics* **2010**, *7*, 605.

(12) Pathak, S. M.; Ruff, A.; Kostewicz, E. S.; Patel, N.; Turner, D. B.; Jamei, M. Model-Based Analysis of Biopharmaceutic Experiments To Improve Mechanistic Oral Absorption Modeling: An Integrated in Vitro in Vivo Extrapolation Perspective Using Ketoconazole as a Model Drug. *Mol. Pharmaceutics* **2017**, *14*, 4305−4320.

(13) Docci, L.; Milani, N.; Ramp, T.; Romeo, A. A.; Godoy, P.; Franyuti, D. O.; Krähenbühl, S.; Gertz, M.; Galetin, A.; Parrott, N.; Fowler, S. Exploration and application of a liver-on-a-chip device in combination with modelling and simulation for quantitative drug metabolism studies. *Lab Chip* **2022**, *22*, 1187−1205.

(14) Chiney, M. S.; Ng, J.; Gibbs, J. P.; Shebley, M. Quantitative Assessment of Elagolix Enzyme-Transporter Interplay and Drug−Drug Interactions Using Physiologically Based Pharmacokinetic Modeling. *Clin. Pharmacokinet.* **2020**, *59*, 617−627.

(15) Reddy, M. B.; Bolger, M. B.; Fraczkiewicz, G.; Del Frari, L.; Luo, L.; Lukacova, V.; Mitra, A.; Macwan, J. S.; Mullin, J. M.; Parrott, N.; Heikkinen, A. T. PBPK Modeling as a Tool for Predicting and Understanding Intestinal Metabolism of Uridine 5'-Diphosphoglucuronosyltransferase Substrates. *Pharmaceutics* **2021**, *13*, 1325.

(16) Parrott, N.; Paquereau, N.; Coassolo, P.; Lave, T. An Evaluation of the Utility of Physiologically Based Models of Pharmacokinetics in Early Drug Discovery. *J. Pharm. Sci.* **2005**, *94*, 2327−2343.

(17) Jones, H. M.; Gardner, I. B.; Watson, K. J. Modelling and PBPK Simulation in Drug Discovery. *AAPS J.* **2009**, *11*, 155.

(18) Naga, D.; Parrott, N.; Ecker, G. F.; Olivares-Morales, A. Evaluation of the Success of High-Throughput Physiologically Based Pharmacokinetic (HT-PBPK) Modeling Predictions to Inform Early Drug Discovery. *Mol. Pharmaceutics* **2022**, *19*, 2203.

(19) Bhhatarai, B.; Walters, W. P.; Hop, C.; Lanza, G.; Ekins, S. Opportunities and challenges using artificial intelligence in ADME/Tox. *Nat. Mater.* **2019**, *18*, 418−422.

(20) Wang, Y.; Liu, H.; Fan, Y.; Chen, X.; Yang, Y.; Zhu, L.; Zhao, J.; Chen, Y.; Zhang, Y. In Silico Prediction of Human Intravenous Pharmacokinetic Parameters with Improved Accuracy. *J. Chem. Inf. Model.* **2019**, *59*, 3968−3980.

(21) Humer, C.; Heberle, H.; Montanari, F.; Wolf, T.; Huber, F.; Henderson, R.; Heinrich, J.; Streit, M. ChemInformatics Model Explorer (CIME): exploratory analysis of chemical model explanations. *Aust. J. Chem.* **2022**, *14*, 21.

(22) Lombardo, F.; Berellini, G.; Obach, R. S. Trend Analysis of a Database of Intravenous Pharmacokinetic Parameters in Humans for 1352 Drug Compounds. *Drug Metab. Dispos.* **2018**, *46*, 1466−1477.

(23) Ye, Z.; Yang, Y.; Li, X.; Cao, D.; Ouyang, D. An Integrated Transfer Learning and Multitask Learning Approach for Pharmacokinetic Parameter Prediction. *Mol. Pharmaceutics* **2019**, *16*, 533−541.

(24) Kratochwil, N. A.; Meille, C.; Fowler, S.; Klammers, F.; Ekiciler, A.; Molitor, B.; Simon, S.; Walter, I.; McGinnis, C.; Walther, J.; Leonard, B.; Triyatni, M.; Javanbakht, H.; Funk, C.; Schuler, F.; Lavé, T.; Parrott, N. J. Metabolic Profiling of Human Long-Term Liver Models and Hepatic Clearance Predictions from In Vitro Data Using Nonlinear Mixed-Effects Modeling. *AAPS J.* **2017**, *19*, 534.

(25) Poulin, P.; Kenny, J. R.; Hop, C. E. C. A.; Haddad, S. In Vitro−In Vivo Extrapolation of Clearance: Modeling Hepatic Metabolic Clearance of Highly Bound Drugs and Comparative Assessment with Existing Calculation Methods. *J. Pharm. Sci.* **2012**, *101*, 838−851.
(26) Williams, R. O.; Watts, A. B.; Miller, D. A. *Formulating Poorly Water Soluble Drugs*; Springer: New York, 2012; Vol. 3.
(27) Di, L. An update on the importance of plasma protein binding in drug discovery and development. *Expert Opin. Drug Discovery* **2021**, *16*, 1453−1465.
(28) Miller, R. R.; Madeira, M.; Wood, H. B.; Geissler, W. M.; Raab, C. E.; Martin, I. J. Integrating the Impact of Lipophilicity on Potency and Pharmacokinetic Parameters Enables the Use of Diverse Chemical Space during Small Molecule Drug Optimization. *J. Med. Chem.* **2020**, *63*, 12156−12170.
(29) Tinworth, C. P.; Young, R. J. Facts, Patterns, and Principles in Drug Discovery: Appraising the Rule of 5 with Measured Physicochemical Data. *J. Med. Chem.* **2020**, *63*, 10091−10108.
(30) Doak, B. C.; Over, B.; Giordanetto, F.; Kihlberg, J. Oral druggable space beyond the rule of 5: insights from drugs and clinical candidates. *Chem. Biol.* **2014**, *21*, 1115−1142.
(31) Young, R. J.; Leeson, P. D. Mapping the Efficiency and Physicochemical Trajectories of Successful Optimizations. *J. Med. Chem.* **2018**, *61*, 6421−6467.
(32) Simulations Plus, I., 1220 W. Avenue J, Lancaster, California 93534-2902, http://www.simulations-plus.com/ Last accessed: 8 Sept, 2022.
(33) Rodgers, T.; Rowland, M. Mechanistic Approaches to Volume of Distribution Predictions: Understanding the Processes. *Pharm. Res.* **2007**, *24*, 918.
(34) Lukacova, V.; Parrott, N. J.; Lavè, T.; Fraczkiewicz, G.; Bolger, M. B.; Woltosz, W. S. General Approach to Calculation of Tissue: Plasma Partition Coefficients for Physiologically Based Pharmacokinetic (PBPK) Modeling. In *Poster Session presented at: 2008 AAPS National Annual Meeting and Exposition*, 2008.
(35) Lukacova, V.; Parrott, N. J.; Lavè, T.; Fraczkiewicz, G.; Bolger, M. B.; Woltosz, W. S. Role of Fraction Unbound in Plasma in Calculations of Tissue: Plasma Partition Coefficients. In *AAPS National Meeting, Atlanta, Georgia*, 2008.
(36) Varma, M.; Steyn, S.; Allerton, C.; El-Kattan, A. Predicting Clearance Mechanism in Drug Discovery: Extended Clearance Classification System (ECCS). *Pharm. Res.* **2015**, *32*, 3785−3802.
(37) Parrott, N.; Lave, T. Applications of Physiologically Based Absorption Models in Drug Discovery and Development. *Mol. Pharmaceutics* **2008**, *5*, 760−775.
(38) Di, L.; Breen, C.; Chambers, R.; Eckley, S. T.; Fricke, R.; Ghosh, A.; Harradine, P.; Kalvass, J. C.; Ho, S.; Lee, C. A.; Marathe, P.; Perkins, E. J.; Qian, M.; Tse, S.; Yan, Z.; Zamek-Gliszczynski, M. J. Industry Perspective on Contemporary Protein-Binding Methodologies: Considerations for Regulatory Drug-Drug Interaction and Related Guidelines on Highly Bound Drugs. *J. Pharm. Sci.* **2017**, *106*, 3442−3452.
(39) Yau, E.; Olivares-Morales, A.; Gertz, M.; Parrott, N.; Darwich, A. S.; Aarons, L.; Ogungbenro, K. Global Sensitivity Analysis of the Rodgers and Rowland Model for Prediction of Tissue: Plasma Partitioning Coefficients: Assessment of the Key Physiological and Physicochemical Factors That Determine Small-Molecule Tissue Distribution. *AAPS J.* **2020**, *22*, 41.
(40) Johnson, T. W.; Gallego, R. A.; Edwards, M. P. Lipophilic Efficiency as an Important Metric in Drug Design. *J. Med. Chem.* **2018**, *61*, 6401−6420.
(41) U.S. Department of Health and Human Services Food and Drug Administration Center for Drug Evaluation and Research (CDER). *In Vitro Drug Interaction Studies Cytochrome P450 Enzyme and Transporter-Mediated Drug Interactions Guidance for Industry*, https://www.fda.gov/media/134582/download (27-Dec-2020), Last accessed: 8 Sept, 2022.
(42) Gleeson, M. P. Plasma protein binding affinity and its relationship to molecular structure: An in-silico analysis. *J. Med. Chem.* **2007**, *50*, 101−112.
(43) Poulin, P.; Theil, F. A priori prediction of tissue: plasma partition coefficients of drugs to facilitate the use of physiologically-based pharmacokinetic models in drug discovery. *J. Pharm. Sci.* **2000**, *89*, 16−35.
(44) Berellini, G.; Waters, N. J.; Lombardo, F. In silico Prediction of Total Human Plasma Clearance. *J. Chem. Inf. Model.* **2012**, *52*, 2069−2078.
(45) Winiwarter, S.; Chang, G.; Desai, P.; Menzel, K.; Faller, B.; Arimoto, R.; Keefer, C.; Broccatell, F. Prediction of Fraction Unbound in Microsomal and Hepatocyte Incubations: A Comparison of Methods across Industry Datasets. *Mol. Pharmaceutics* **2019**, *16*, 4077−4085.
(46) Yang, J.; Jamei, M.; Yeo, K. R.; Rostami-Hodjegan, A.; Tucker, G. T. Misuse of the Well-Stirred Model of Hepatic Drug Clearance. *Drug Metab. Dispos.* **2007**, *35*, 501−502.
(47) Rodgers, T.; Leahy, D.; Rowland, M. Physiologically Based Pharmacokinetic Modeling 1: Predicting the Tissue Distribution of Moderate-to-Strong Bases. *J. Pharm. Sci.* **2005**, *94*, 1259−1276.
(48) Uchimura, T.; Kato, M.; Saito, T.; Kinoshita, H. Prediction of human blood-to-plasma drug concentration ratio. *Biopharm. Drug Dispos.* **2010**, *31*, 286−297.
(49) Korzekwa, K.; Nagar, S. Drug Distribution Part 2. Predicting Volume of Distribution from Plasma Protein Binding and Membrane Partitioning. *Pharm. Res.* **2017**, *34*, 544−551.

https://doi.org/10.1021/acs.molpharmaceut.2c00350
Mol. Pharmaceutics XXXX, XXX, XXX−XXX